REGULARIZED QUADRATURE AND PHASE TRACKING (RQPT) FROM A SINGLE CLOSED-FRINGE INTERFEROGRAM

Manuel Servin, José Luis Marroquín and Juan Antonio Quiroga

Comunicación Técnica No I-03-13/05-08-2003
(CC/CIMAT)

Regularized Quadrature and Phase Tracking (RQPT) from a single closed-fringe interferogram

Manuel Servin
Jose Luis Marroquin*
Juan Antonio Quiroga**

Centro de Investigaciones en Optica A. C. (CIO)
Apartado Postal 1-948
37150 Leon, Gto., Mexico
*Centro de Investigaciones en Matematicas A. C. (CIMAT)
Apartado Postal 402
36000 Guanajuato, Gto., Mexico
**Departamento de Optica, Universidad Complutense de Madrid,
Ciudad Universitaria S/N, 2841 Madrid Spain
Madrid, Spain

Abstract

A new sequential phase demodulator based on a Regularized Quadrature and Phase Tracking system (RQPT) is applied to demodulate two-dimensional fringe patterns. This RQPT system tracks the fringe pattern's quadrature and phase in a sequential way following the path of the fringes. To make the RQPT system more robust to noise the modulating phase around a small neighborhood is modeled as a plane and the quadrature of the signal is estimated simultaneously with the fringe's modulating phase. By sequentially calculating the quadrature of the fringe pattern one obtains a more robust sequential demodulator than it was previously possible. This system may be applied to the demodulation of a single interferogram having closed-fringes.

1 Introduction

Most experimental data obtained using full field optical metrology are encoded as a wavefront (phase) which modulates the fringes of an interferometric image [1]. The aim of fringe analysis is to estimate the modulating two-dimensional phase of these fringe patterns. When a linear spatial phase with a large slope (a carrier) is added to the wavefront under analysis one obtains a spatial carrier frequency interferogram. When the interesting phase is smooth and a linear carrier is added, the fringe pattern can be easily demodulated using well understood and widely used spatial carrier interferometry techniques [2].

On the other hand, if the experiment at hand permits one to obtain several interferograms over a period of time, one may introduce a temporal carrier to the modulating phase [3]. In this case one varies the modulating phase using a linear temporal carrier so every interferogram will have a predefined piston phase difference. Then, using several phase stepped interferograms, one may easily obtain the modulating phase.

Sometimes, however, the very nature of the experimental set-up may not allow one to take one or several interferometric images having spatial and/or temporal carrier [4]. These cases frequently arise in the analysis of fast transient phenomena, where it is difficult or impossible to introduce spatial or temporal carrier. In these cases we have no other choice but to deal with a single or a series of interferograms without carrier, possibly containing closed fringes, where the phase variation is not a monotonic function of space or time. In this situation it is impossible separate the interesting information using a linear filter. However there are still some possible ways to deal with these non-monotonic modulating phase interferograms. One recent method was proposed by Larkin *et.al* [5] and more recently, another closely related to that one by Servin *et. al.* [6]. In these two cases the phase estimation problem is factored into two operators. One is an isotropic two-dimensional 2-D Hilbert transform and the other one is the orientation 2π of the fringes. The orientation of the fringes is the most difficult step and must be done in a sequential way [7]. The Regularized Quadrature and Phase Tracker (RQPT) system presented herein uses instead a single system which is capable of demodulating in a robust way a *single* interferogram containing closed fringes.

The Regularized Quadrature and Phase Tracker (RQPT) presented in this work may be considered as a significant improvement to a previously published phase demodulation system called the Regularized Phase Tracker or

RPT [8]. The improvement resides on the sequential quadrature estimation of the interferogram's fringes by the RQPT. Although the main objective of any fringe pattern demodulation technique is to find the modulating phase, it is interesting to note (as we will see) that the sequential calculation of the interferogram's quadrature highly improves the robustness of the RPT system presented in past publications. So this new RQPT sequentially calculates the quadrature of the fringe pattern as a by-product to obtain a phase tracking scheme that is more robust than the previous RPT demodulation algorithm.

The presentation plan for the paper is the following: in section 2.1 we review the Phase Locked Loop (PLL) [9] which is the first one-dimensional (1D) sequential phase demodulator used to analyze two-dimensional (2D) interferograms because an important idea which is used in the RQPT is drawn directly from the PLL system. The motivation for a non-regularized Quadrature and Phase Tracker QPT demodulation system in 1D is presented in section 2.2. In section 3 this 1D non-regularized (QPT) system is generalized to 2D. In section 4 we regularize the QPT to obtain the searched 2D Regularized-QPT or RQPT. We continue to section 5 where we demodulate an experimentally obtained Electronic Speckle Interferogram and then a complicated, noisy, computer-generated fringe pattern. In section 6 some conclusions of the main results of the paper are given.

2 Sequential phase demodulating systems

In this section we present the motivation for a 1D non-regularized Quadrature and Phase Tracker (QPT) demodulation system. In section 3 this 1D non-regularized QPT system is generalized to 2D. And finally in section four we regularize the QPT to obtain the searched RQPT. We begin by describing the standard model for a two dimensional fringe pattern as obtained by an optical interferometer,

$$I(\mathbf{r}) = a(\mathbf{r}) + b(\mathbf{r})cos[\phi(\mathbf{r})] \tag{1}$$

where $\mathbf{r} = (x, y)$ represents a point in the two dimensional space. The smooth function $a(\mathbf{r})$ is a low frequency signal and represents the background illumination. The function $b(\mathbf{r})$ is also a low frequency signal which represents the two dimensional contrast variation of the fringe pattern. The signal $\phi(\mathbf{r})$

is the information to be recovered which is related with the physical magnitude under measurement. Throughout this work we will assume that the modulating phase $\phi(\mathbf{r})$ is continuous and smooth.

Let us start by analyzing the Phase Locked Loop (PLL), which was the first phase tracking system that was applied to fringe pattern demodulation [9]. A brief reviewing of the PLL is convenient because the herein presented QPT uses a fundamental idea which is drawn directly from the PLL system. Afterwards we show why the PLL system is not suitable for demodulating a single closed-fringe interferogram. We continue our presentation by analyzing another phase tracking system which is now suitable for demodulating wide band low frequency signals, therefore overcoming the main limitation faced by the PLL to demodulate fringe patterns modulated by a non-monotonic phase $\phi(\mathbf{r})$. Near the final part of the paper we propose a regularization technique for the QPT system to obtain the new Regularized Sequential Quadrature and Phase (RQPT) estimator.

2.1 The Phase Locked Loop (PLL) System

As we will see, both the PLL and the RQPT systems are capable of demodulating *only* open fringe patterns if no attention is paid to the 2D sequential scanning strategy. Let us start with an analysis of a one dimensional carrier frequency signal and how the PLL and the RQPT system presented in this work demodulate it. The standard mathematical model for a one dimensional fringe pattern with linear carrier is the following,

$$I_1(x) = a(x) + b(x)\cos[\omega_0 x + \phi(x)] \tag{2}$$

the carrier frequency ω_0 must be greater than the maximum frequency content of the modulating phase $\phi(x)$ or $\omega_0 > |\partial\phi(x)/\partial x|$ for all x. The PLL (as well as the RQPT) work best when the background signal is removed or it is highly attenuated. Then using a high pass filter one is able to rewrite Eq.2 as

$$I(x) = b(x)\cos[\omega_0 x + \phi(x)] \tag{3}$$

the continuous first order Phase Locked Loop system is usually described by the following nonlinear dynamic system:

$$\frac{d\hat{\phi}(x)}{dx} = \tau I(x)\sin[\omega_0 x + \hat{\phi}(x)] \tag{4}$$

where $\hat{\phi}(x)$ denotes the estimated modulating phase, and τ is a constant related to the band pass of the PLL. To understand the basic functioning of this system, let us rewrite the last equation in integral form as:

$$\hat{\phi}(x) = \tau \int_{-\infty}^{x} \cos[\omega_0 \xi + \phi(x)] \sin[\omega_0 \xi + \hat{\phi}(\xi)] \, d\xi \tag{5}$$

where we have assumed that we have $b(x) \approx 1.0$. This equation may be rewritten as:

$$\hat{\phi}(x) = \tau \int_{-\infty}^{x} \Big(\sin[\phi(\xi) - \hat{\phi}(\xi)] + \sin[2\omega_0 \xi + \hat{\phi}(\xi) + \phi(\xi)] \Big) \, d\xi \tag{6}$$

as we can see from this equation there are two terms; the first one varies slowly because the modulating phase $\phi(x)$ is a continuous smooth function, while the second one varies twice as fast as the original fringes. Because the integral is a first order low pass filter, the fast varying term is highly reduced and may be neglected. Therefore one may rewrite, for analysis purposes, a simplified version for the PLL dynamic system as:

$$\frac{d\hat{\phi}(x)}{dx} = \tau \sin[\phi(x) - \hat{\phi}(x)] \tag{7}$$

when the PLL is operating in lock, the estimated phase $\hat{\phi}(x)$ follows the modulating phase $\phi(x)$ very closely so the difference $\phi(x) - \hat{\phi}(x)$ is small and the sine function may be approximated by its argument. Doing this we finally arrive to

$$\frac{d\hat{\phi}(x)}{dx} = \tau [\phi(x) - \hat{\phi}(x)] \tag{8}$$

this last approximation enables one to understand why the demodulated phase $\hat{\phi}(x)$ obtained by using a first order PLL follows closely the modulating phase of the fringes $\phi(x)$

Finally let us write the spatially discretized (or digital) version of the PLL system which is obtained by discretizing the spatial coordinate x. Using first order differences to approximate the continuous phase derivative one obtains a digital first order PLL as,

$$\hat{\phi}(x+1) = \hat{\phi}(x) + \tau I(x) \sin[\omega_0 x + \hat{\phi}(x)] \tag{9}$$

With this equation one sees that the currently evaluated phase $\hat{\phi}(x+1)$ at the site $x+1$ uses the previously estimated phase $\hat{\phi}(x)$ as a predictor with an

update given by $\tau I(x)\sin[\omega x + \hat{\phi}(x)]$ which corrects the preceding estimate by a small amount. Finally, let us mention that the phase estimated by the PLL is already unwrapped, so that no additional unwrapping system is required to obtain the searched smooth modulating phase.

We have seen that the PLL system is capable of demodulating a carrier frequency signal whenever we have an estimate of the carrier frequency ω_0, and the two terms in Eq.6 are well separated in the frequency space. If the spectral distance between these two terms is not enough, they overlap and the higher frequency carrier will appear as an artifact in the estimated phase. This situation arises if a low frequency carrier is modulated by a wide-band phase and in this case it is not possible to use the PLL system to demodulate these fringes. We will see in the next section the new phase tracking demodulator (the QPT) which overcomes these difficulties.

2.2 The Quadrature and Phase Tracker (QPT) estimator system

Let us start by intuitively motivating how one can arrive to another phase tracking scheme which overcomes the PLL system limitations. In this case instead of starting with a dynamic system and then explaining why does it work as in the case of the PLL, we will proceed by postulating a cost functional operating over the estimated phase space $\hat{\phi}(x)$, hoping that the solution $\hat{\phi}(x)$ which render this functional minimum is the expected demodulated phase.

For this let us naively postulate a very simple quadratic cost functional that we know the searched solution will render minimum. This cost functional is,

$$U = [I(x) - \cos(\hat{\phi}(x))]^2 \tag{10}$$

where we have simplified our one dimensional fringe pattern model assuming that $a(x) \approx 0$ and $b(x) \approx 1$. The optimum function is obtained by the signal,

$$\hat{\phi}(x) = \arccos[I(x)] \tag{11}$$

such a phase is illustrated in Fig.1(a), and it is clear that this is not what we were looking for. Then, let us continue working over the same idea by introducing another term to our cost functional that imposes an additional constraint on $\hat{\phi}(x)$ by requiring that one also approximates the quadrature of the fringes. The quadrature of $I(x) = \cos[\phi(x)]$ is $\sin[\phi(x)] = -I_x(x)/\phi_x(x) =$

$-I_x(x)/\omega_(x)$, where $\omega(x)$ is the local frequency. With this addition our new cost functional now reads,

$$U = [I(x) - \cos(\hat{\phi}(x))]^2 + [I_x(x) + \hat{\omega}(x)\sin(\hat{\phi}(x))]^2 \tag{12}$$

where the new unknown function $\hat{\omega}(x)$ is the derivative of $\hat{\phi}(x)$ with respect to x, and $I_x(x)$ is approximated by first order differences as $I(x) - I(x-1)$ in our discrete one-dimensional space. Now the optimum for $\hat{\omega}(x)$ and $\hat{\phi}(x)$ is obtained and the solution looks as Fig.1(b). This solution was found iteratively and following the gradient of U with respect to the optimizing variables. That is,

$$\hat{\phi}(x)^{k+1} = \hat{\phi}(x)^k - \mu\frac{\partial U}{\partial\hat{\phi}(x)} \tag{13}$$

$$\hat{\omega}(x)^{k+1} = \hat{\omega}(x)^k - \mu\frac{\partial U}{\partial\hat{\omega}(x)} \tag{14}$$

where μ is a fixed step size. If one uses "natural" (given that we do not know anything about $\phi(x)$ or $\hat{\omega}(x)$) zero initial conditions

$$\hat{\phi}(x)^0 = 0\ , \qquad \hat{\omega}(x)^0 = 0 \tag{15}$$

one obtains the estimated phase and local frequency shown in Fig.1(b); it is apparent that we have made no progress towards the desired solution: we just found what we already knew from our first attempt. The reason for this is that although we have added another datum which is $I_x(x)$ we also have added a new unknown which is $\hat{\omega}(x)$ so we have returned at our starting point.

If we could have a rough estimate for the newly created unknown $\hat{\omega}(x)$, however, introducing this value into our last cost functional, one would be closer to knowing the quadrature of the fringes at site x. One way to obtain this rough estimate, is by using the same PLL trick, namely, to use the previously found estimate (in this case for $\hat{\omega}(x)$) at the already visited site $x-1$ as our initial guess. Using as initial estimate $\hat{\omega}(x)^0 = \hat{\omega}(x-1)^\infty$ in Eq.14, one gets a better estimate for the searched $\hat{\phi}(x)$ that was previously possible. Once a better $\hat{\phi}(x)$ is found we then use it to improve our estimate for the actual $\hat{\omega}(x)$, which in turn is used to improve our $\hat{\phi}(x)$. We may continue this iterative process until we find both unknowns within a certain predefined error. By doing this one obtains the searched (wrapped) demodulated phase.

Of course the very first site being demodulated within the fringe pattern will not have a "previously found estimation"; for that unique "seed" site the initial conditions for $\hat{\phi}(x)$ and $\hat{\omega}(x)$ may be set to zero.

Another alternative explanation that supports the use of the stable estimated $\hat{\omega}(x-1)^{\infty}$ as initial condition for $\hat{\omega}(x)^0$ may be found by observing the unwanted behavior that the local frequency $\hat{\omega}(x)$ has when zero initial conditions are chosen for Eq.14 (Fig.1-b). The desired estimated frequency $\hat{\omega}(x)$ should be a constant and not a square function. The discontinuities of $\hat{\omega}(x)$ are due to the fact that the driving term $\partial U/\partial\hat{\omega}(x)$ (in Eq.14) has a very low value on the neighborhood of the extrema of the fringe pattern. In these places only the driving term for $\hat{\phi}(x)$ which is $\partial U/\partial\hat{\phi}(x)$ has a significant value and pulls down the estimated phase in the absence of a driving "force" for the instantaneous frequency $\hat{\omega}(x)$. So $\hat{\omega}(x)$ does not have any other choice but to "follow" the changes commanded by the estimated phase $\hat{\phi}(x)$, which finally switches $\hat{\omega}(x)$ to a constant negative value. To get out from this situation one should use as initial condition for $\hat{\omega}(x)^0$ (in Eq.14) the stable value for $\hat{\omega}(x-1)^{\infty}$ found at the previously visited site $x-1$. In this way instead of having a negligible value for $\hat{\omega}(x)$ it will have as initial estimate the value $\hat{\omega}(x-1)^{\infty}$ which is a significant positive value. In that case the natural solution for the estimated phase at x is to continue its monotonically increasing behavior (see Fig.1c). Once this critical point has been "jumped" by this trick the driving term $\partial U/\partial\hat{\omega}(x)$ will have again a high and well determined value, forcing the frequency $\hat{\omega}(x)$ to remain positive until the next critical point of the fringe pattern appears.

We may also use the previous estimation at $\hat{\phi}(x-1)$ as initial guess for $\hat{\phi}(x)$ as is done in the PLL. This process of using the two previously found estimates for $\hat{\phi}(x)$ and $\hat{\omega}(x)$ enables us not only to find the searched phase and frequency at x but also to unwrap the phase being demodulated as in the PLL case. In summary the sequential Quadrature and Phase Tracking (QPT) system is still given by Eqs.13-14 but now the initial conditions to be used are:

$$\hat{\phi}(x)^0 = \hat{\phi}(x-1)^{\infty}\ , \qquad \hat{\omega}(x)^0 = \hat{\omega}(x-1)^{\infty} \tag{16}$$

where $\hat{\omega}(x-1)^{\infty}$ and $\hat{\phi}(x-1)^{\infty}$ denote the stable point $(\hat{\phi},\hat{\omega})$ of the previously demodulated site at $x-1$. Using these initial conditions one now obtains the expected continuous phase. Summarizing the QPT system has two important advantages over the PLL: one is that no carrier frequency estimate is needed, and second, one does not have to worry about the risk of having overlapping

spectra as was the case for the PLL system.

3 Demodulation of 2D closed fringe patterns using the sequential Quadrature and Phase Tracker(QPT) estimator

Before further discussion, let us generalize our 1D-QPT to two dimensions. This generalization is straight forward and is obtained by minimization of the following cost functional,

$$U = [I - \cos(\hat{\phi})]^2 + [I_x + \hat{\omega}_x \sin(\hat{\phi})]^2 + [I_y + \hat{\omega}_y \sin(\hat{\phi})]^2 \tag{17}$$

where the spatial position dependence $\mathbf{r} = (x, y)$ of $I_x,\ I_y,\ \hat{\phi},\ \hat{\omega}_x,\ \hat{\omega}_y$ was omitted for clarity purposes. Now we need to optimize for three functions namely $\hat{\phi},\ \hat{\omega}_x,\ \hat{\omega}_y$. The optimizing system at the site $\mathbf{r}_i$ has a similar form to that of the 1D-QPT system, in this case we have,

$$\hat{\phi}(\mathbf{r}_i)^{k+1} = \hat{\phi}(\mathbf{r}_i)^k - \mu \frac{\partial U}{\partial \hat{\phi}(\mathbf{r}_i)} \tag{18}$$

$$\hat{\omega}_x(\mathbf{r}_i)^{k+1} = \hat{\omega}_x(\mathbf{r}_i)^k - \mu \frac{\partial U}{\partial \hat{\omega}_x(\mathbf{r}_i)} \tag{19}$$

$$\hat{\omega}_y(\mathbf{r}_i)^{k+1} = \hat{\omega}_y(\mathbf{r}_i)^k - \mu \frac{\partial U}{\partial \hat{\omega}_y(\mathbf{r}_i)} \tag{20}$$

with initial conditions given by,

$$\hat{\phi}(\mathbf{r}_i)^0 = \hat{\phi}(\mathbf{r}_{i-1})^\infty\ ,\ \hat{\omega}_x(\mathbf{r}_i)^0 = \hat{\omega}_x(\mathbf{r}_{i-1})^\infty\ ,\ \hat{\omega}_y(\mathbf{r}_i)^0 = \hat{\omega}_y(\mathbf{r}_{i-1})^\infty \tag{21}$$

where $\mathbf{r}_i$ is the current i site under optimization, and $\mathbf{r}_{i-1}$ is the previous one. In the 2D-QPT case the two dimensional fringe signal can be demodulated whenever

$$\|\hat{\omega}(\mathbf{r})\| = \left[\hat{\omega}_x^2(\mathbf{r}) + \hat{\omega}_y^2(\mathbf{r})\right]^{1/2} > 0 \tag{22}$$

according to the last equation the 2D-PT system will successfully demodulate open low frequency fringes regardless of their two-dimensional orientation.

We have seen that the QPT system can demodulate carrier frequency fringe patterns without the need of an explicit linear carrier. As we have also seen this has the advantage of demodulating very low frequency fringes

without worrying of higher frequency cross-tacking signals as in the PLL case. But how can this 2D-QPT system be used to demodulate closed fringe interferograms where the spatial phase variation is non-monotonic, since the 2D-QPT only demodulates monotonically increasing phase ? the answer is: *following the path of the fringes*. That is, not in a row by row scanning strategy (as in a television set), but following the path traced by the fringes themselves. One way of achieving this is using an algorithm published in [10] which uses the concept of signal "quality". This scanning strategy was originally used to sequentially unwrap noisy phase maps. This algorithm first classifies regions of the image according to how good the signal to noise ratio is around a given neighborhood. In that case [10] one starts the sequential unwrapping algorithm by first unwrapping the best data (less noisy), and afterwards the noisier image regions.

In our 2D-QPT case we are not classifying our data as function of its signal to noise ratio. We simply assign in an arbitrary way that our data will have two qualities which are:

$$if \quad I(x) > 0 \text{ ; good data} \tag{23}$$

$$if \quad I(x) \leq 0 \text{ ; bad data} \tag{24}$$

this is shown, for example in Fig.3a and Fig.3b. Using this arbitrary classification (actually the negative of the above statement could also have been used) coupled with the "quality" following scanning strategy [10] one is able to follow preferably a scanning path defined by the fringes [8]. The main and essential advantage of following the fringes is to avoid crossing straight through the critical points of the modulating phase. The reason is that the 2D-QPT system does not estimate the local curvature of the modulating phase (only its value and gradient), so the 2D-QPT does not know how to handle the variety of critical points (minima, maxima or saddles). In contrast, if the 2D-QPT system continually follows the fringe path it always "sees" open fringes all over the two-dimensional interferogram. In other words, scanning the interferogram along the fringe paths behaves roughly like a coordinate transformation where closed fringes are transformed into open fringes. Therefore whenever the 2D-QPT system encircles these critical points the 2D-QPT system will never "know" that it was actually demodulating a closed fringe interferogram. Eventually, after demodulating the neighborhood (at a small distance) of these critical points, the 2D-QPT will finally have to deal with them. In those critical regions the local gradient

$\|\hat{\omega}(\mathbf{r})\|$ is almost zero so the only remaining term in the functional is the first one. However delicate, in this final step of the demodulation process the problem is much less severe given that we have already demodulated the phase surrounding these critical points and the solution will grow towards the remaining un-demodulated region in a robust way.

This fringe following 2D-QPT algorithm makes use of the local geometry of the phase being recovered by modeling the local phase $\hat{\phi}(\mathbf{r})$ by a small one-pixel-plane determined by the triad $\hat{\phi}$, $\hat{\omega}_x$, $\hat{\omega}_y$. Additionally, the fringe following 2D-QPT also has global information of the phase at its disposal and uses it by scanning the interferogram following its fringes.

Figure 2 shows some snap shots on the QPT demodulating process. We can see how the 2D fringe pattern is being phase demodulated following the fringe scanning strategy. As also can be seen, the critical points are not processed until its surrounding phase is already demodulated. In this case we have obtained the path-following data (Fig.2b) by splitting the fringe's gray-level range into four regions instead of just two as in Eqs.23-24

4 Regularizing the Quadrature and Phase Tracker (RQPT) estimator

In the previous section we have shown how the sequential Quadrature and Phase Tracker (QPT) may be used to demodulate closed fringe interferograms modulated by a smooth continuous function. However the QPT system just presented is not at all robust with respect to noise. To improve the QPT robustness we need to regularize the cost functional. In classical regularization one normally introduces a smoothing term in the cost functional. The smoothing term is normally built using integrals of derivative operators applied to the field that one wants to recover [11]. This is the standard way of regularizing an inverse linear problem when the transforming linear operator is not invertible or is ill-conditioned. Another characteristic of classical regularization algorithms is that the functional used to find the inverse field is optimized globally at each iteration. That is, one updates all the sites within the region Ω where one wants to recover the inverse field at each global iteration. In contrast, in the QPT case one is finding the modulating phase and the fringe's quadrature sequentially. So one cannot use differential operators to regularize the QPT functional. Fortunately one can find a way to regular-

ize this functional by assuming that within a neighborhood (ϵ, η) around the point (x, y) one may model the modulating phase as a plane. So one takes as a parametric model for the local phase in the neighborhood of (x, y) the plane given by,

$$p(\epsilon, \eta) = \hat{\phi}(x, y) + \hat{\omega}_x(x, y)(x - \epsilon) + \hat{\omega}_y(x, y)(y - \eta) \tag{25}$$

using this plane model the local functional looks like,

$$U = \sum_{(\epsilon,\eta)\in N_{x,y}} \left\{ [I - \cos(p)]^2 + [I_x + \hat{\omega}_x \sin(p)]^2 + [I_y + \hat{\omega}_y \sin(p)]^2 \right\} \tag{26}$$

where we have omitted the (x, y, ϵ, η) dependance for clarity purposes. Now the optimization proceeds not just taking into account only the current site (x, y) but a two-dimensional neighborhood $N_{x,y}$ around it. The size of the neighborhood normally used varies from a 3X3 up to an 11X11 pixel window or more depending on the signal to noise ratio of the interferogram. The larger the size of the fitting plane $p(x, y)$ the better noise rejection is obtained. Of course the size of the fitting plane is limited by how reasonable is to consider the interferogram's phase within the neighborhood $(\epsilon, \eta) \in N_{x,y}$ as a plane. Finally, one may still increase a little bit more the RQPT noise robustness by adding another term which measures the distance between the regularizing plane $p(x, y)$ and previously estimated values of demodulated phase $\hat{\phi}(\epsilon, \eta)$ within $N_{x,y}$. With this last addition the non-linear cost functional is,

$$U = \sum_{(\epsilon,\eta)\in N_{x,y}} \left\{ [I - \cos(p)]^2 + [I_x + \hat{\omega}_x \sin(p)]^2 + [I_y + \hat{\omega}_y \sin(p)]^2 + \lambda(\hat{\phi} - p)^2 m \right\} \tag{27}$$

where the function $m(\epsilon, \eta)$ is an indicator function which has value of 1 when the site at (ϵ, η) has already been estimated and of 0 otherwise. The parameter λ is a regularization parameter which controls, along with the size of the regularizing plane, the highest frequency content of the demodulated signal $\hat{\phi}(x, y)$. The value of the λ parameter is not very critical; for example all numerical experiments that we have made use $\lambda = 5$ with good results.

5 Experimental and simulation results

We show in Fig.3 the application of the RQPT system for demodulating an experimentally obtained speckle fringe pattern. Again we show in this

figure some snap-shots in the demodulating process, to see how the sequential strategy along the fringes is performed. Although the noise in this fringe pattern is moderately high, the fringe pattern is not "too complicated". That is, it does not contain many fringes nor many critical points. So in this case a large 13X13 neighborhood pixel may be used. This large fitting plane filters out efficiently the noise of the estimated phase.

No fringe analysis system is "noise immune"; sooner or later a noise energy is reached such that the fringe demodulation system breaks down and gives a useless estimated phase. Of course the RQPT system is not an exception. So, in the next example (Figure 4) we have simulated a more complicated noisy fringe pattern with a non constant modulation $b(x, y)$ and zero background $a(x, y) = 0$. The aim of this simulation is to stretch the RQPT robustness to the limit in terms of noise and fringe complication. As occurs with any other fringe pattern demodulation system the RQPT may demodulate very noisy fringe patterns whenever the fringes are "not so complicated", i.e. it may have high noise but few fringes and few critical points. On the contrary a fringe pattern cannot be "too noisy" when a more complicated fringe pattern containing many fringes and many critical points (minima, maxima or saddle) is analyzed such as the one shown in figure 4a. Also in Fig.4 we show some other signals involved in the phase estimation process. Figure 4b shows the path along the fringes that the RQPT will follow preferentially. Figure 4c shows the quadrature signal obtained by this sequential system. If the noise and/or the fringe pattern is more complicated that the one shown in Fig.4 it is advised to use as a first step in the demodulation process a robust two-dimensional filtering and normalizing algorithm before making use of the RQPT.

6 Comparison between the RPT and the RQPT systems

We have analyzed the RQPT system and we have seen how it can be used to demodulate closed-fringe interferograms. In this section the RQPT system is compared to the RPT [8] system and explicitly point out the advantages of the RQPT. In the case of demodulating a computer-generated noise-free fringe pattern both systems give the expected continuous and smooth modulating phase even for a small regularizing neighborhood $N_{x,y}$. The advantage

of the RQPT system becomes clearer when a noisy interferogram is analyzed. In this section we show experimentally how the RQPT system is more robust to noise and to fluctuations in the fringe contrast $b(x, y)$ than the RPT system. The reason is that the RQPT system has the additional constraint term related with the quadrature of the data signal.

Let us begin by displaying the local cost functionals for both sequential demodulating systems. For the RPT the local cost functional is:

$$U_{RPT} = \sum_{(\epsilon,\eta)\in N_{x,y}} \Big\{ [I - \cos p]^2 + \lambda(\hat{\phi} - p)^2 m \Big\} \tag{28}$$

and the one corresponding to the RQPT system is:

$$U_{RQPT} = \sum_{(\epsilon,\eta)\in N_{x,y}} \Big\{ [I - \cos p]^2 + [I_x + \hat{\omega}_x \sin p]^2 + [I_y + \hat{\omega}_y \sin p]^2 + \lambda(\hat{\phi} - p)^2 m \Big\} \tag{29}$$

where in both cases the regularizing plane is given by

$$p(\epsilon, \eta) = \hat{\phi}(x) + \hat{\omega}_x(x, y)(x - \epsilon) + \hat{\omega}_x(x, y)(y - \eta) \tag{30}$$

One can see that the difference between these cost functionals is the quadrature related term which is $U_Q = [I_x - \hat{\omega}_x \sin(p)]^2 + [I_y - \hat{\omega}_y \sin(p)]^2$. Although it may look as a minor addition, it has nevertheless important consequences in terms of robustness to noise and rejection of undesired solutions.

As mentioned, the problem of estimating the modulating phase of a single interferogram containing closed fringes is ill-posed, because this problem has infinitely many solutions compatible with the observations. However, the fact that in the minimizing algorithms (RPT or RQPT) one uses the final state of a neighborhood pixel as the initial condition of the pixel being demodulated, shrinks the solution space to the set of continuous functions. As a consequence the two main competing continuous solutions which render both local functionals to low values are:

$$\hat{\phi}_1(x) \approx \phi(x, y), \tag{31}$$

$$\hat{\phi}_2(x) \approx \cos^{-1}[I(x, y)], \tag{32}$$

where $\cos^{-1}(\cdot)$ is the inverse of $\cos(\cdot)$ and takes values in the closed interval $[0, \pi]$. These two solutions are continuous functions compatible with the observed data. Of course the solution given by $\hat{\phi}_1(x)$ (Fig.1c) is smoother than $\hat{\phi}_2(x)$ (Fig.1a) so the regularizing plane biases the RPT/RQPT systems

towards $\hat{\phi}_1(x)$. However, in noisy situations, the noisy estimate of $\hat{\phi}_1$ may fall too close to $\hat{\phi}_2$ and the RPT system may fail to recover the desired solution $\hat{\phi}_1(x)$. On the other hand the RQPT system has two additional constraint terms which adds robustness to the system and gives the expected minimum $\hat{\phi}_1$ in many cases where the RPT fails.

One example of the higher robustness of the RQPT over the RPT system may be seen in a contrast miss-match situation between the fringe model and the fringe data. In Figure 5a we show the following simple noise-free computer-generated fringe pattern:

$$I(x, y) = 0.8 \cos(\omega_0 x) \tag{33}$$

In this case the RPT system finds the competing solution $\hat{\phi}_2$ because the RPT fails to reach near the phase values of 0 or π which would allow it to "jump" between adjacent Riemann surfaces corresponding to $\cos^{-1}(\cdot)$ to obtain $\omega_0 x$ instead of obtaining $\hat{\phi} = \cos^{-1}[I(x, y)]$ (Fig.5b) as a solution. So in this case the RPT remains on a single branch of the Riemann surface regardless of the size of the neighborhood $N_{x,y}$. On the other hand the RQPT finds the desired solution $\omega_0 x$ (Fig.5c) because this system implicitly calculates the quadrature of the fringes. In this numerical experiment (Fig.5) we have used a neighborhood $N_{x,y} = 5$ and the parameter $\lambda = 5$ for both the RPT and the RQPT systems. Note that, if the amplitude's fringe model and the actual fringe amplitude diverge even further in this direction, i.e. $I(x, y) = 0.5 \cos(\omega_0 x)$, maintaining a normalized fringe model, both systems fail to recover the desired function $\omega_0 x$.

In the next example we consider the noisy interferogram:

$$I(x, y) = cos[\omega_0 x + n(x, y)] \tag{34}$$

Here we have a perfect match between the data and the fringe model's contrast. However, in this case we have added some phase noise $n(x, y)$. This noise is uniformly distributed in the range $[-1, 1]$ radians. Fig.6a shows the fringe pattern, and Figs.6b and 6c, the demodulated phase obtained by the RPT and the RQPT systems respectively. As one can see, the RQPT obtains a good approximation of the desired phase $\omega_0 x$, while the RPT obtains again the wrong solution $\cos^{-1}[\cos(\omega_0 x)]$. In this numerical experiment we have used a neighborhood $N_{x,y} = 9$ and the parameter $\lambda = 5$ for both the RPT and the RQPT systems.

It should be noted that in [8], it was proposed to introduce an additional term to the RPT cost functional, in order to increase the robustness with respect to noise, the resulting cost functional is:

$$U_{RPT} = \sum_{(\epsilon,\eta)\in N_{x,y}} \left\{ [I - \cos p]^2 + [I - \cos(p+\alpha)]^2 + \lambda(\hat{\phi} - p)^2 m \right\} \qquad (35)$$

where α is a piston phase shift (usually $\alpha = \pi/4$) introduced to the fringe model. This is a rather awkward constraint that forces the phase shifted model also to resemble the original fringe data. Although this trick may permit one to obtain a solution in the correct branch of the Reimann surface in noisy interferograms, it nevertheless distorts the resulting phase estimation. That is because the 2 terms cannot be made equal to zero simultaneously. So a compromise between them is taken and this compromise is the expected demodulated signal slightly distorted. In the RPT paper [8] it is advised that after the distorted phase is obtained, this distortion may be removed by minimizing the "unshifted" functional (28) taking as initial condition the optimum $\hat{\phi}(x)$ obtained from the "phase shifted" functional (35). This heuristic trick is not necessary in the RQPT system presented in this work.

7 Conclusions

We have shown that the estimation of the local phase of the fringe pattern may be made more robust and stable if the quadrature of the fringe pattern — which depends on its gradient and local frequency — is estimated at the same time. This estimation process is effective only if the phase variation is locally monotonic, i.e., if the fringes are (locally) open. It is possible however, to use this scheme to estimate the phase of patterns with closed fringes as well, provided one scans the image in such a way that the demodulator always "sees" an open fringe pattern, and has a good initial estimate of its phase and local frequency. This will not be the case, of course, of critical points (maxima, minima, saddles) of the phase surface, but if these difficult spots are demodulated after the phase has been estimated at all their surrounding pixels, the QPT operator will obtain a correct value there as well. We have also shown that the QPT estimator may be made robust to noise by estimating the parameters of a linear (planar) approximation to the phase surface in a neighborhood, instead of the phase and frequency values at the point, obtaining in this case the RQPT. The robustness with respect to noise

improves if the size of this neighborhood is increased, but its maximum size is limited by the smoothness of the underlying phase surface, i.e. the size of the larger window where a linear approximation to the phase remains valid.

The RQPT system may have difficulties in demodulating even noise free fringe patterns having some of their critical points near or at the boundary of the fringe pattern. That is because at these places there are no closed paths around the critical points and the main strategy of surrounding the critical points by following the fringes may fail.

Finally we have made a detailed comparison between the herein presented RQPT system with the previously published RPT [8] demodulator. We have stressed their similarities and differences, and made it clear that the RQPT is the next logical step for the improvement of the RPT.

Acknowledgement

M. Servin and J. L. Marroquin were partially supported by grants 33429-E and 34575A respectively from Consejo Nacional de Ciencia y Tecnologia (CONACYT), Mexico.

References

1.- D. Malacara, M. Servin, Z. Malacara, *Interferogram Analysis for Optical Testing*, Chap. 1, (Marcel Dekker, New York, 1998)

2.- M. Takeda,, H. Ina, and S. Kobayashi, "Fourier-Transform method of fringe pattern analysis" J. Opt. Soc. Am. **72**, 156-160 (1982)

3.- D. Malacara, M. Servin, Z. Malacara, *Interferogram Analysis for Optical Testing*, Chap. 6, (Marcel Dekker, New York, 1998)

4.- G. Cloud, *Optical methods of Engineering Analysis* (Cambridge U. Press, Cambridge UK. 1995)

5.- K. G. Larkin, D. J. Bone, and M. A. Oldfield, "Natural demodulation of two-dimensional fringe patterns. I. General Background of the spiral phase quadrature transform," J. Opt. Soc. Am. A **18**, 1862-1870 (2001).

6.- M. Servin, J. A. Quiroga, and J. L. Marroquin, "General n-dimensional Quadrature transform and its application to interferogram demodulation," J. Opt. Soc. Am. A **20**, 925-934 (2003).

7.- J. A. Quiroga, M. Servin, F. J. Cuevas, "Modulo 2π fringe orientation angle estimation by phase unwrapping with a regularized phase tracking algorithm," J. Opt. Soc. Am. A **19**, 1524-1531 (2002).

8.- M. Servin, J. L. Marroquin, and F. J. Cuevas, "Fringe-follower regularized phase tracker for demodulation of closed-fringe interferograms," J. Opt. Soc. Am. **18** 689-695 (2001).

9.- M. Servin, R. Rodriguez-Vera, "Two dimensional phase locked loop demodulation of carrier frequency interferograms," J. Mod. Opt. *40*, 2087-2094 (1993).

10.- B. Ströbel, "Processing of interferometric phase maps as complex-valued phasor images," Appl. Opt. **35**, 2192-2198 (1996).

11.- C. W. Groetsch, *Inverse Problems in the Mathematical Sciences* (Vieweg and Sohn, Braunschweig, Germany, 1993).

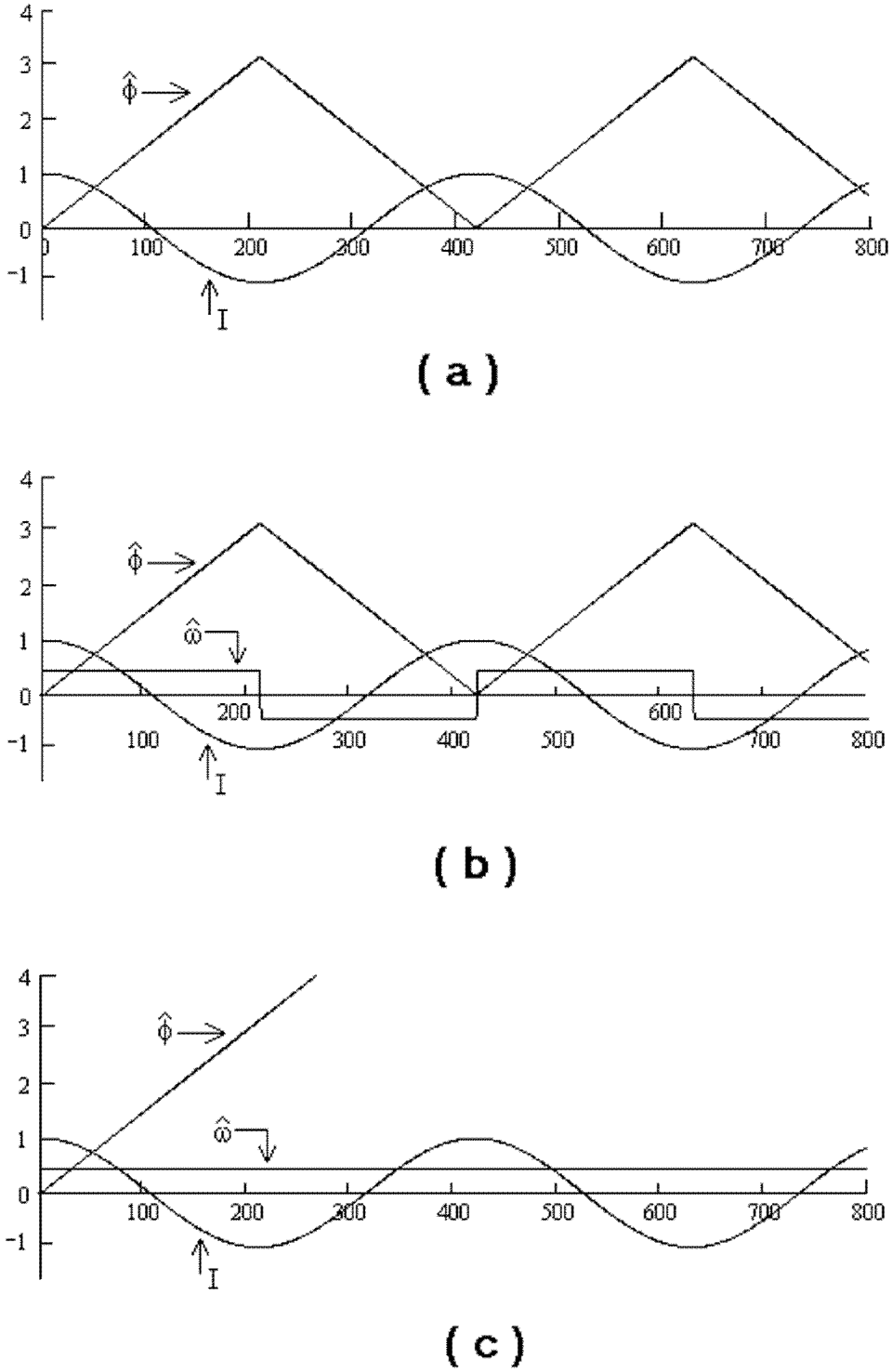

Figure 1: Phase demodulation of a sinusoidal signal. (a) Estimated phase given by $\hat{\phi} = \cos^{-1}(\phi)$ which is the minimum of U in Eq.10.(b) Minimizing function of Eq.12 along with zero initial conditions (Eq.15). (c) The function which minimizes Eq.12 but now using as initial conditions the previously found estimates (Eq.16, QPT)

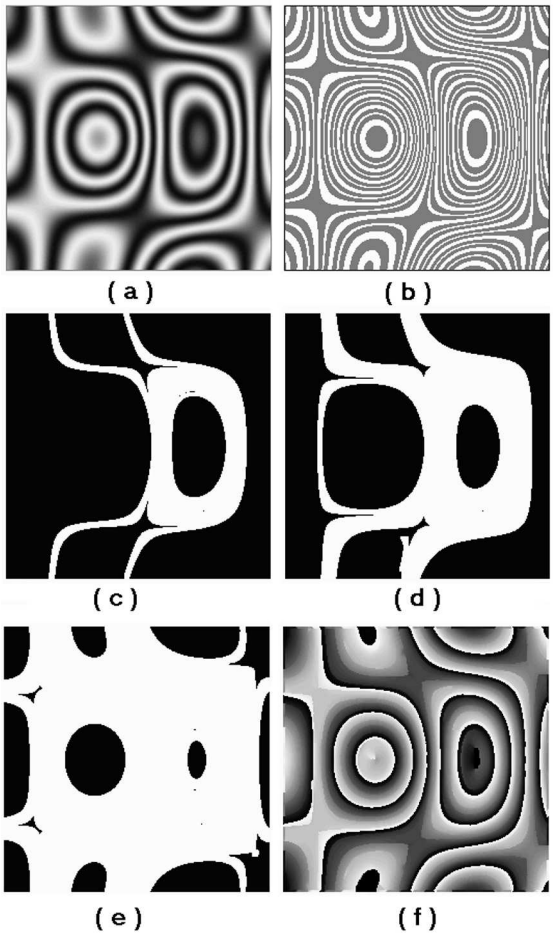

Figure 2: Demodulation of a two-dimensional fringe pattern using the non-regularized Quadrature and Phase (QPT) estimator. (a) The given noiseless computer generated fringe pattern. (b) The path followed by the sequential demodulating system. Whiter paths are preferably followed as being the sites with "higher quality". (c)(d)(e) Path demodulation progress of the QPT system. (f) Demodulated phase. Although the QPT demodulator finds the phase unwrapped, the phase was re-wrapped to compared it with panel (a).

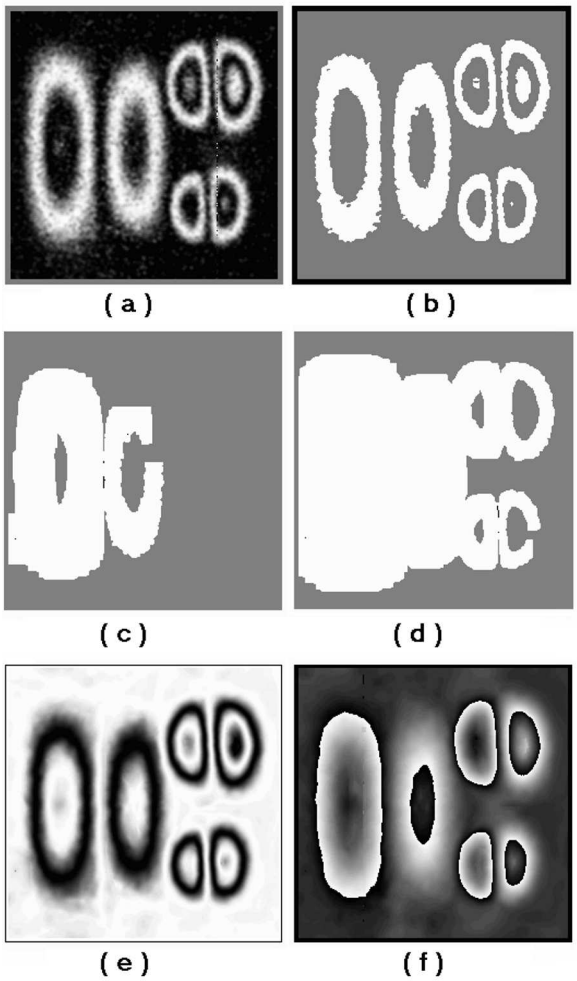

Figure 3: Phase demodulation of an experimentally obtained speckle interferometric pattern. (a) The speckle pattern. (b) The traced path that the Regularized-QPT (RQPT) demodulating system follows. Whiter zones are preferably first demodulated. (c) and (d) two "moments" on the path followed by the RQPT demodulating system. (e) The quadrature of the original fringe pattern. (f) The demodulated phase shown re-wrapped.

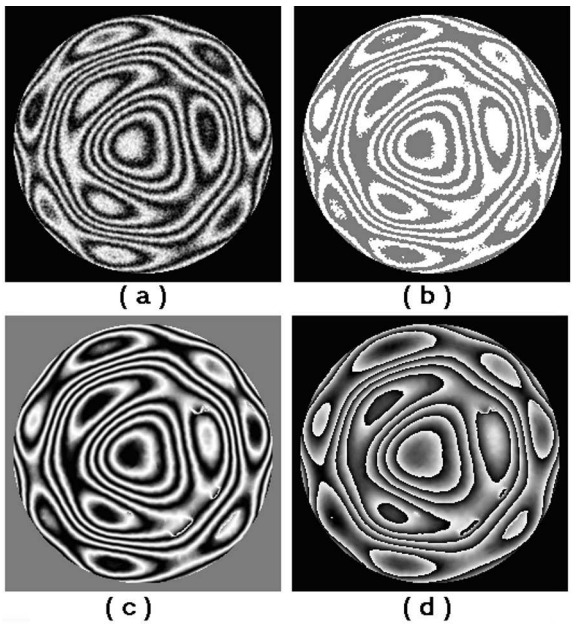

Figure 4: Phase demodulation of a noisy computer generated fringe pattern. (a) The noisy fringe pattern.(b) The traced path that the sequential RQPT demodulating system will follow. Whiter zones are preferably first demodulated. (c) The quadrature of the original fringe pattern. (d) The demodulated phase shown re-wrapped.

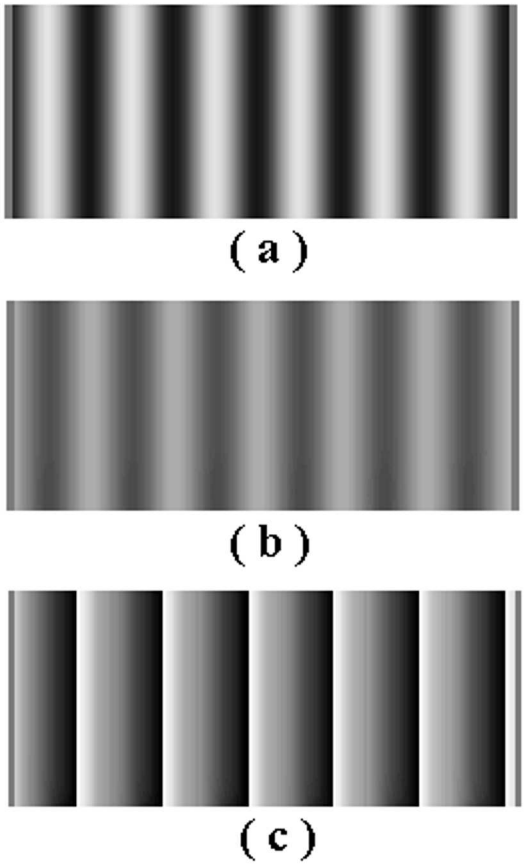

Figure 5: Phase demodulation of a fringe pattern with less than expected fringe contrast of 1.0. (a) The fringe pattern data, $I(x) = 0.8\cos(\omega_0 x)$. (b) Wrong demodulated phase found by the RPT Eq.28 which is close to $\hat{\phi}(x) = \cos^{-1}[I(x)]$. (c) Correctly demodulated phase using the RQPT system.

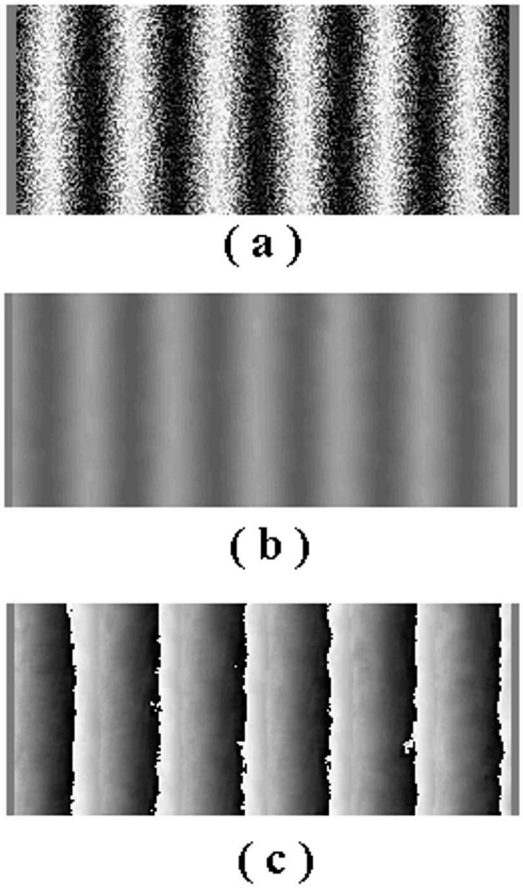

Figure 6: Phase demodulation of a noisy fringe pattern with the right (expected) contrast equal to 1.0. (a) The noisy fringe pattern $I(x) = \cos[\phi(x) + noise(x)]$. (b) Wrong demodulated phase using the RPT system given by Eq.28 which is close to $\hat{\phi}(x) = \cos^{-1}[I(x)]$. (c) The correctly demodulated phase obtained by the RQPT system.